Ultraviolet-visible conical emission by multiple laser filaments

P. Maioli[1,*], R. Salamé[1], N. Lascoux[1], E. Salmon[1], P. Béjot[2], J. Kasparian[1,2], and J.-P. Wolf[2]

[1]Université de Lyon, Université Lyon 1, CNRS, LASIM UMR 5579, bâtiment A. Kastler, 43 boulevard du 11 novembre 1918, F-69622 Villeurbanne, France
[2]GAP-Biophotonics, University of Geneva, 20 rue de Médecine, Geneva 1211, Switzerland
[*]Corresponding author: paolo.maioli@lasim.univ-lyon1.fr

Abstract: We characterized the angular distribution of the supercontinuum emission from multiple infrared laser filaments propagating in air over long distances, from the infrared (1080 nm) to ultraviolet (225 nm). These experimental data suggest that the X-Waves modeling or Cerenkov emission, rather than phase matching of four-wave mixing, could explain the conical emission. We also estimate the total light conversion efficiency from the original laser wavelength into the white-light continuum.

OCIS codes: (190.7110) Ultrafast nonlinear optics; (320.6629) Supercontinuum generation; (190.5940) Self-action effects; (260.5950); Self-focusing

References and links

1. L. Bergé, S. Skupin, R. Nuter, J. Kasparian, and J.-P. Wolf, "Ultrashort filaments of light in weakly ionized, optically transparent media," Rep. Prog. Phys. **70**, 1633-1713 (2007).
2. S. L. Chin, S. A. Hosseini, W. Liu, Q. Luo, F. Théberge, N. Aközbek, A. Becker, V. P. Kandidov, O. G. Kosareva, and H. Schroeder, "The propagation of powerful femtosecond laser pulses in optical media: physics, applications, and new challenges," Can. J. Phys. **83**, 863-905 (2005).
3. A. Couairon and A. Mysyrowicz, "Femtosecond filamentation in transparent media," Phys. Rep. **441**, 47-189 (2007).
4. J. Kasparian and J.-P. Wolf, "Physics and applications of atmospheric nonlinear optics and filamentation," Opt. Express **16**, 466-493 (2007).
5. J. Kasparian, M. Rodriguez, G. Méjean, J. Yu, E. Salmon, H. Wille, R. Bourayou, S. Frey, Y-B. André, M. Franco, B. Prade, A. Mysyrowicz, and R. Sauerbrey, "White-light filaments for atmospheric analysis," Science **301**, 61-64 (2003).
6. H. Pépin, D. Comtois, F. Vidal, C. Y. Chien, A. Desparois, T. W. Johnston, J. C. Kieffer, B. La Fontaine, F. Martin, F. A. M. Rizk, C. Potvin, P. Couture, H. P. Mercure, A. Bondiou-Clergerie, P. Lalande, and I. Gallimberti, "Triggering and guiding high-voltage large-scale leader discharges with sub-joule ultrashort laser pulses," Phys. Plasmas **8**, 2532-2539 (2001).
7. X. M. Zhao, J.-C. Diels, C. Y. Wang, and M. Elizondo, "Femtosecond ultraviolet laser pulse induced lightning discharges in gases," IEEE J. Quantum Electron. **31**, 599-612 (1995).
8. G. Méjean, R. Ackermann, J. Kasparian, E. Salmon, J. Yu, and J.-P. Wolf, "Improved laser triggering and guiding of megavolt discharges with dual fs-ns pulses," Appl. Phys. Lett. **88**, 021101 (2006).
9. J. Kasparian, R. Ackermann, Y.-B. André, G. Méchain, G. Méjean, B. Prade, P. Rohwetter, E. Salmon, K. Stelmaszczyk, J. Yu, A. Mysyrowicz, R. Sauerbrey, L. Wöste, and J.-P. Wolf, "Electric events synchronized with laser filaments in thunderclouds," Opt. Express **16**, 5757-5763 (2008).
10. R. R. Alfano and S. L. Shapiro, "Observation of Self-Phase Modulation and Small-Scale Filaments in Crystals and Glasses," Phys. Rev. Lett. **24**, 592-594 (1970).
11. A. Brodeur and S. L. Chin, "Ultrafast white-light continuum generation and self-focusing in transparent condensed media," J. Opt. Soc. Am. B **16**, 637-650 (1999).
12. A. L. Gaeta, "Catastrophic Collapse of Ultrashort Pulses," Phys. Rev. Lett. **84**, 3582-3585 (2000).
13. P. Béjot, J. Kasparian, and J.-P. Wolf, "Cross-compression of light bullets by two-color co-filamentation," Phys. Rev A **78**, 043804 (2008).
14. C. D'Amico, A. Houard, M. Franco, B. Prade, A. Mysyrowicz, A. Couairon, and V. T. Tikhonchuk, "Conical Forward THz Emission from Femtosecond-Laser-Beam Filamentation in Air," Phys. Rev. Lett. **98**, 235002 (2007).

#102431 - $15.00 USD Received 9 Oct 2008; revised 6 Nov 2008; accepted 18 Nov 2008; published 10 Mar 2009

15. H. Xiong, H. Xu, Y. Fu, Y. Cheng, Z. Xu, and S. L. Chin, "Spectral evolution of angularly resolved third-order harmonic generation by infrared femtosecond laser-pulse filamentation in air," Phys. Rev. A **77**, 043802 (2008).
16. M. Kolesik, E. M. Wright, A. Becker, and J. V. Moloney, "Simulation of third-harmonic and supercontinuum generation for femtosecond pulses in air," Appl. Phys. B **85**, 531-538 (2006).
17. M. Kolesik, E. M Wright, and J. V. Moloney, "Supercontinuum and third-harmonic generation accompanying optical filamentation as first-order scattering processes," Opt. Lett. **32**, 2816-2818 (2007).
18. H. Wille, M. Rodriguez, J. Kasparian, D. Mondelain, J. Yu, A. Mysyriwicz, R. Sauerbrey, J.-P. Wolf, and L. Wöste, "Teramobile: A mobile femtosecond-terawatt laser and detection system," Eur. Phys. J. Appl. Phys. **20**, 183-190 (2002).
19. G. Méjean, J. Kasparian, J. Yu, E. Salmon, S. Frey, J.-P. Wolf, S. Skupin, A. Vinçotte, R. Nuter, S. Champeaux, and L. Bergé, "Multifilamentation transmission through fog," Phys. Rev. E **72**, 026611 (2005).
20. E. T. J. Nibbering, P. F. Curley, G. Grillon, B. S. Prade, M. A. Franco, F. Salin, and A. Mysyrowicz, "Conical emission from self-guided femtosecond pulses in air," Opt. Lett. **21**, 62-64 (1996).
21. O. G. Kosareva, V. P. Kandidov, A. Brodeur, and S. L. Chin, "Conical emission from laser plasma interactions in the filamentation of powerful ultrashort laser pulses in air," Opt. Lett. **22**, 1332-1334 (1997).
22. I. Golub, "Optical characteristics of supercontinuum generation," Opt. Lett. **15**, 305-307 (1990).
23. Q. Xing, K. M. Yoo, and R. R. Alfano, "Conical emission by four-photon parametric generation by using femtosecond laser pulses," Appl. Opt. **32**, 2087-2089 (1993).
24. G. G. Luther, A. C. Newell, J. V. Moloney, and E. M. Wright, "Short-pulse conical emission and spectral broadening in normally dispersive media," Opt. Lett. **19**, 789-791 (1994).
25. M. Kolesik, E. M. Wright, and J. V. Moloney, "Dynamic Nonlinear X Waves for Femtosecond Pulse Propagation in Water," Phys. Rev. Lett. **92**, 253901 (2004).
26. D. Faccio, M. Porras, A. Dubietis, F. Bragheri, A. Couairon, and P. Di Trapani, "Conical Emission, Pulse Splitting, and X-Wave Parametric Amplification in Nonlinear Dynamics of Ultrashort Light Pulses," Phys. Rev. Lett. **96**, 193901 (2006).
27. D. Faccio, A. Averchi, A. Lotti, P. Di Trapani, A. Couairon, D. Papazoglou, and S. Tzortzakis, "Ultrashort laser pulse filamentation from spontaneous XWave formation in air," Opt. Express **16**, 1565-1570 (2008).
28. G. Méjean, J. Kasparian, J. Yu, S. Frey, E. Salmon, J.-P. Wolf, L. Bergé, and S. Skupin, "UV–Supercontinuum generated by femtosecond pulse filamentation in air: Meter-range experiments versus numerical simulations," Appl. Phys. B **82**, 341-345 (2006).
29. L. Bergé, S. Skupin, G. Méjean, J. Kasparian, J. Yu, S. Frey, E. Salmon, and J.-P. Wolf, "Supercontinuum emission and enhanced self-guiding of infrared femtosecond filaments sustained by third-harmonic generation in air," Phys. Rev. E. **71**, 016602 (2005).
30. M. Rodriguez, R. Bourayou, G. Méjean, J. Kasparian, J. Yu, E. Salmon, A. Scholz, B. Stecklum, J. Eislöffel, U. Laux, A. P. Hatzes, R. Sauerbrey, L. Wöste, and J.-P. Wolf, "Kilometer-range nonlinear propagation of femtosecond laser pulses," Phys. Rev. E **69**, 036607 (2004).
31. S. Skupin, L. Bergé, U. Peschel, F. Lederer, G. Méjean, J. Yu, J. Kasparian, E. Salmon, J.-P. Wolf, M. Rodriguez, L. Wöste, R. Bourayou, and R. Sauerbrey, "Filamentation of femtosecond light pulses in the air: Turbulent cells versus long-range clusters," Phys. Rev. E **70**, 046602 (2004).
32. E.R. Peck and K. Reeder, "Dispersion of Air," J. Opt. Soc. Am. **62**, 958-962 (1972).
33. D. Faccio, A. Averchi, A. Couairon, M. Kolesik, J. V. Moloney, A. Dubietis, G. Tamosauskas, P. Polesana, A. Piskarskas, and P. Di Trapani, "Spatio-temporal reshaping and X Wave dynamics in optical filaments," Opt. Express **15**, 13077-13095 (2007).
34. D. Faccio, A. Lotti, M. Kolesik, J. V. Moloney, S. Tzortzakis, A. Couairon, and P. Di Trapani, "Spontaneous emergence of pulses with constant carrier-envelope phase in femtosecond filamentation," Opt. Express **16**, 11103-11114 (2008).
35. M. Aldener, S. S. Brown, H. Stark, J. S. Daniel, and A. R. Ravishankara, "Near-IR absorption of water vapor: Pressure dependence of line strengths and an upper limit for continuum absorption," J. Mol. Spectrosc. **232**, 223-230 (2005).
36. S. Roy, T. R. Meyer, and J. R. Gord, "Broadband coherent anti-Stokes Raman scattering spectroscopy of nitrogen using a picosecond modeless dye laser," Opt. Lett. **30**, 3222-3224 (2005).
37. F. Théberge, M. Châteauneuf, V. Ross, P. Mathieu, and J. Dubois, "Ultrabroadband conical emission generated from the ultraviolet up to the far-infrared during the optical filamentation in air," Opt. Lett. **33**, 2515-2517 (2008).

1. Introduction

Propagation of high energy femtosecond laser beams in the atmosphere has drawn a considerable attention both for the study of fundamental characteristics of filaments [1-4] and for the development of many applications like atmospheric remote sensing [5] or triggering and guiding of electric discharges in the prospect of lightning control [6-9]. Femtosecond intense laser pulses can propagate in the atmosphere over several Rayleigh lengths as self-

#102431 - $15.00 USD Received 9 Oct 2008; revised 6 Nov 2008; accepted 18 Nov 2008; published 10 Mar 2009

guided filaments. The basic mechanism of self-guiding consists of a dynamic balance between the nonlinear Kerr effect in air, which self-focuses the beam until ionization of oxygen molecules by multiphoton absorption, and the defocusing effect of plasma, which prevents optical collapse and sustains long-distance propagation. Besides this basic image, many nonlinear physical processes accompany filamentation, e.g. spectral broadening by self-phase modulation [10, 11], self-compression [12, 13], generation of THz radiation [14] or third-harmonic generation [15-17]. Moreover, when the pulse power largely exceeds the critical power (P_{crit} ~ 3 GW in air at 800 nm), multiple filamentation occurs [18], with a number of filaments proportional to the power [19].

A visually spectacular effect associated with filamentation is conical emission [20, 21]. It generates a wealth of coloured rings around the beam in the forward direction, whose peak wavelength decreases from infrared to ultraviolet with increasing distance from the propagation axis. The mechanism at the root of conical emission is still debated. It may imply Cerenkov radiation [20, 22], self-phase modulation (SPM) [21], four-wave mixing (FWM) [23, 24] or X-Waves modelling [25-27]. The first experimental measurements of conical emission in air have been performed in the 500-700 nm range [20, 21]. More recently, Méjean *et al*. estimated a divergence of the UV conical emission, although this estimation was based on indirect observation [28, 29]. In addition, the first high-resolution angle-wavelength spectrum of air filaments and the link with X-Waves was recently introduced [27].

In this Letter, we extend the measurement of conical emission to the ultraviolet, down to 225 nm. Moreover, we show that conical emission is not modified by multiple filamentation, as had been suggested based on indirect observations [30].

2. Experimental setup

Figure 1 shows the experimental setup. Intense femtosecond pulses at λ_0 = 800 nm (FWHM 23 nm) were generated by the Teramobile facility [18] whose laser system consists of a Ti:Sa oscillator followed by a chirped pulse amplification (CPA) chain. The compressed pulses, of 100 fs pulse duration at a 10 Hz repetition rate, had energies of 305 mJ. The corresponding peak power is 3 TW, *i.e.* 1000 P_{crit}, which yields a few tens of filaments. The amplified femtosecond beam, with an initial diameter of 15 cm, was focused by a sending telescope (f = +42 m), leading to a filamentation onset at z_{f1} = 30 m and a filamentation length of 22 m until z_{f2} = 52 m. Downstream of the filaments, at z = 82.5 m, 86 m and 106 m respectively, we measured the forward-emitted spectrum as a function of the transverse distance from the beam center, hence of the emission angle θ over ± 8 mrad. At each angle, the spectrum was recorded between 225 and 1080 nm with 0.4 nm resolution by a computer-interfaced spectrometer (OceanOptics HR2000+), whose input optical fiber was oriented toward the incoming laser source and swept across the beam profile.

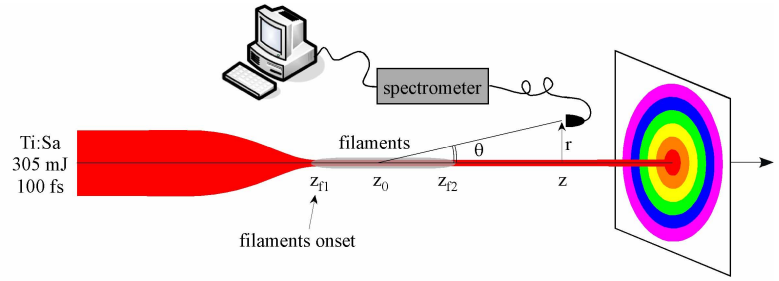

Fig. 1. Experimental setup. A fiber collector is swept across the beam downstream of the filamenting region and the collected conical emission is analyzed on a spectrometer.

To correctly record the spectra in spite of their high dynamics (8 orders of magnitude), we employed different neutral filters with high optical density (up to OD 4.0) and varied the integration time from 1 s to 65 s (10 to 650 laser shots). For most of the positions, we acquired

#102431 - $15.00 USD Received 9 Oct 2008; revised 6 Nov 2008; accepted 18 Nov 2008; published 10 Mar 2009

at least two spectra: one with higher optical density and shorter integration time, to avoid saturation when measuring the intense 800 nm peak, and another with lower densities and longer integration times, for resolving very weak conical emission features at remote wavelengths. Data were smoothed by running averages over 10 adjacent points, *i.e.* over 4 nm.

3. Results and discussion

The data recorded at distances $z = 82.5$ m, 86 m and 106 m yield consistent angles if considering that the origin of the conical emission lies at $z_0 = 44.5$ m, which lies equally spaced between z_{f1} and z_{f2}, *i.e.* in the middle of the filamenting region. This suggests that conical emission is generated all along the filamenting region, a picture consistent with the dynamical replenishment model, in which relatively short filaments are generated randomly all along the filamenting region [31] and independently emit conical emission.

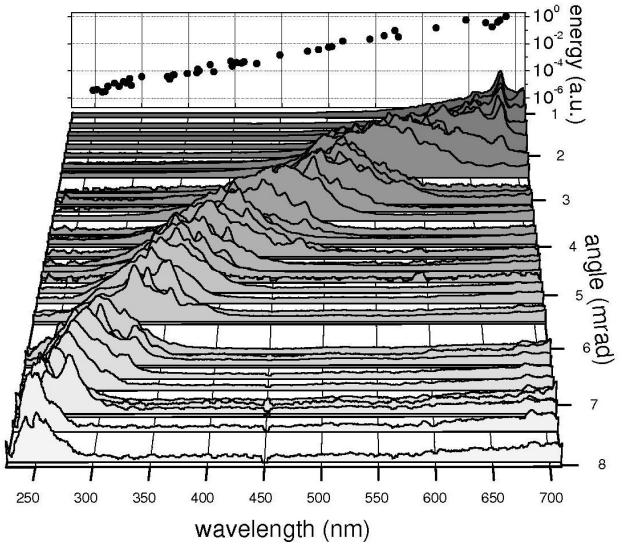

Fig. 2. Main graph: Normalized light intensity spectra as a function of angle θ with respect to the axis of propagation. The spectral dependence of conical emission angle is clearly visible (see also Fig. 3). Back panel: integrated energy of the conical emission as a function of wavelength.

Figure 2 displays the forward-emitted spectra over the 225-710 nm region as a function of θ. Each spectrum is independently normalized to unity. The energy of the conical emission peak is also displayed as a function of wavelength on the rear panel of Fig. 2. It is obtained by integrating the intensity of the un-normalized spectra over the wavelength as well as spatially over the ring (i.e., over 2π on the azimuthal angle). The peak of conical emission shifts from 250 nm up to the fundamental wavelength, and broadens from 20 to 140 nm (FWHM inferred from Lorentzian fits) for decreasing values of θ. Note that no conical emission was observed in the infrared between 800 and 1080 nm.

Figure 3 displays the wavelength dependence of the conical emission, as extracted from Fig. 2. Our data agree well with previous ones obtained in the case of single filamentation by Nibbering *et al.* [20] and Kosareva *et al.* [21] between 500 and 700 nm. In particular, the conical emission angle decreases regularly with increasing wavelength. Note that our measurements are a convolution of the emission angles from individual filaments and of the divergence of the filament bundle. Due to the overall beam refocusing near the focus [30], this divergence is smaller than initial geometrical beam divergence of 1.8 mrad (half angle), but could not be quantitatively determined in our experiment. This error shall be below $\Delta\theta = 1$ mrad, in line with observations over longer distances [30]. Hence, our data show that

#102431 - $15.00 USD Received 9 Oct 2008; revised 6 Nov 2008; accepted 18 Nov 2008; published 10 Mar 2009

the indirect measurements of Méjean *et al.* [28, 29] underestimated the conical emission angles, especially in the 300 - 450 nm range, by approximately 2 mrad. The origin of this underestimation could lie in an improper modelling of their Lidar geometrical compression.

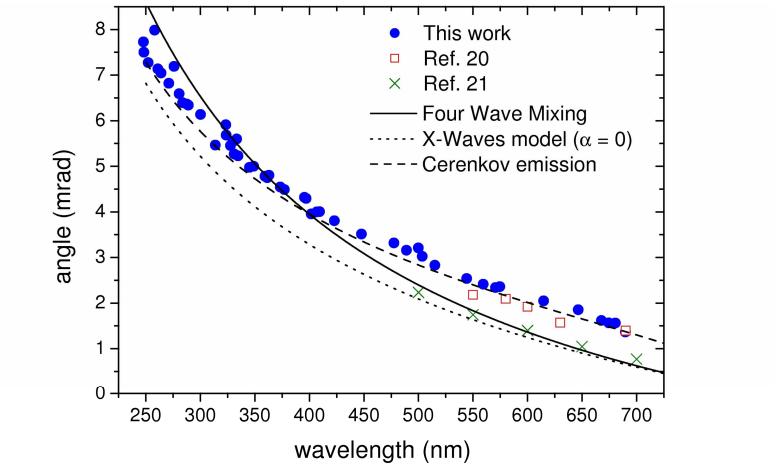

Fig. 3. Conical emission angle versus central wavelength.

We compared our data with the respective angular dispersion of conical emission predicted by FWM [24], X-Waves stationary solutions [27] and by the Cerenkov emission interpretation [20]. In the case of FWM, phase matching imposes the following angular dispersion of conical emission:

$$\theta = \sqrt{k_0'' / k_0}\,\Omega, \tag{1}$$

where $k(\omega) = n(\omega)\omega / c$ ($\omega = 2\pi c / \lambda$ being the frequency and *n(ω)* the refractive index of air, given by [32]), $\Omega = \omega - \omega_0$ is the difference between the generated frequency and the input pump frequency and $k_0^n = \partial^n k(\omega) / \partial \omega^n \big|_{\omega_0}$ [24]. On the other hand, according to the X-Waves solution theory [27], the angle θ is given by:

$$\theta = \sqrt{1 - \left(\frac{k_0 + \Omega / v_g}{k(\omega)} \right)^2} \approx 1 - \frac{1}{2k(\omega)^2} \left(k_0 + \frac{\Omega}{v_g} \right)^2, \tag{2}$$

where $v_g = 1/(k_0' - \alpha)$ is the filament group velocity and α is a free fit parameter which accounts for the input conditions [33], which we set to zero in our curve. This is equivalent to considering $v_g = 1/k_0' \equiv v_c$, where v_c is the laser pulse group velocity at the carrier frequency. In the case of Cerenkov emission [20], the same dispersion relation writes:

$$\cos(\theta) = \frac{1}{k(\omega)} \left(k_0 + \frac{n_0}{c} \Omega \right). \tag{3}$$

Note that by introducing the series expansion $\cos(\theta) = (1 - \theta^2 + \ldots)^{1/2}$ in Eq. (3) we obtain the same approximate expression as in Eq. (2) for the particular case $v_g = c / n_0 \equiv v_\phi$. In other words, the Cerenkov relation can be considered as a sub-case of the more general X-Waves relation when the filament group velocity v_g equals the carrier frequency phase velocity v_ϕ. While the three models fit the previous data adequately, our extension of the data to the UV partially lifts the ambiguity. Our data show that the measured CE spectra are well reproduced by using the Cerenkov expression, *i.e.* by putting $v_g = v_\phi$ in the X Waves relation [34]. On the other hand, the FWM predicts a slope significantly different from that of the experimental

#102431 - $15.00 USD Received 9 Oct 2008; revised 6 Nov 2008; accepted 18 Nov 2008; published 10 Mar 2009

data, especially under 450 nm. Our measurements therefore suggest that the latter process alone is not sufficient to fit data. In addition, when points are shifted downward to correct for the beam divergence ($\Delta\theta \leq 1$ mrad), X-Waves dispersion relation of Eq. (2) always fits the data precisely by using a value of α ranging from 0 to $2 \cdot 10^{-14}$ s/m.

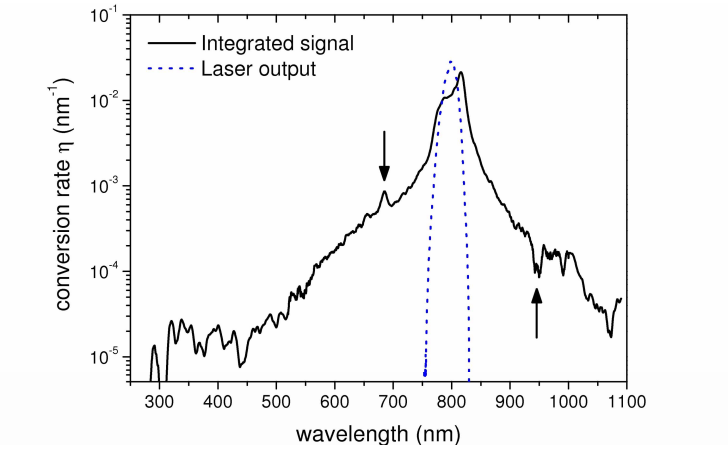

Fig. 4. Conversion efficiency from the fundamental wavelength into white light. Arrows point coherent anti-Stokes Raman scattering (CARS) emission and water vapor absorption.

By integrating the intensity spectra over the full θ angle distribution *i.e.* from -8 to 8 mrad, and normalizing by the total beam energy, we calculated for the first time the absolute conversion efficiency from the fundamental wavelength of the incident laser into the white-light continuum. Fig. 4 displays the conversion efficiency rate per spectral unit, $\eta(\lambda)$, expressed in nm^{-1}, which describes the amount of the incident energy at 800 nm which is converted into an infinitesimal wavelength range centered at λ (resolution 4 nm). The spectrum after propagation is centered at 806 nm, slightly red-shifted as compared with the incident carrier wavelength at 800 nm. In addition, it features both the water vapor absorption line at 940 nm (3ν polyad vibrational states of H_2O) [35] and the coherent anti-Stokes Raman scattering (CARS) emission of N_2 at 678 nm, corresponding to a Raman shift of 2329 cm^{-1} from the 806 nm central wavelength [36]. The observation of these spectral features illustrates the capability of the supercontinuum to provide a suitable light source for both absorption and Raman spectroscopy in the atmosphere.

4. Conclusion

As a conclusion, we have characterized the conical emission from multiple filamentation down to 225 nm in the ultraviolet. The data prolong well the previously existing ones, while we observed no conical emission between 800 and 1080 nm. Our data exclude the phase-matching of FWM as the only mechanism driving conical emission in the UV, and favor X-Waves modeling and Cerenkov emission. They are also useful for applications which require a good characterization of the emission geometry, such as white-light Lidar.

Acknowledgments

The authors acknowledge funding from the Agence Nationale de la Recherche (ANR, grant # NT05-1_43175), Fonds national suisse de la recherche scientifique (FNS, grants #200021-111688/1 and 200021-116198/1), and the Swiss Secrétariat d'État à l'Éducation et à la Recherche in the framework of the COST P18 project "The physics of Lightning Flash and its Effects".

Note: after acceptance of this paper, we became aware of complementary measurements of conical emission in the infrared up to 14 μm [37].

#102431 - $15.00 USD Received 9 Oct 2008; revised 6 Nov 2008; accepted 18 Nov 2008; published 10 Mar 2009